Label-free imaging of lymph nodes with stimulated Raman scattering microscopy

Yuanzhen Suo, Wenlong Yang, Fake Lu, Xiaoliang Sunney Xie

Yuanzhen Suo, Wenlong Yang, Fake Lu, Xiaoliang Sunney Xie, "Label-free imaging of lymph nodes with stimulated Raman scattering microscopy," Proc. SPIE 11190, Optics in Health Care and Biomedical Optics IX, 111900J (20 November 2019); doi: 10.1117/12.2536264

SPIE.

Event: SPIE/COS Photonics Asia, 2019, Hangzhou, China

Label-free Imaging of Lymph Nodes with Stimulated Raman Scattering Microscopy

Yuanzhen Suo[a,b], Wenlong Yang[c,e], Fake Lu[c,f], Xiaoliang Sunney Xie*[a,b,d]
[a]Biomedical Pioneering Innovation Center, Peking University, 5 Yiheyuan Road, Beijing, China; [b] School of Life Sciences, Peking University, 5 Yiheyuan Road, Beijing, China; [c]Department of Chemistry and Chemical Biology, Harvard University, 12 Oxford Street, Cambridge, Massachusetts, MA USA 02138; [d]Beijing Advanced Innovation Center for Genomics, Peking University, Beijing 100871, China; [e]Current position: Center for Advanced Imaging, Harvard University, 52 Oxford Street, Cambridge, Massachusetts, MA USA 02138; [f]Current position: Department of Biomedical Engineering, Binghamton University, 4400 Vestal Parkway E, Binghamton, New York, NY USA 13902

ABSTRACT

Lymph nodes are an important secondary lymphoid organ in the lymphatic system. It is the major site of B cells, T cells and other white blood cells, leading to the function of identifying and fighting infection. To observe the structure of the lymph node, it is necessary to label it with dyes or fluorescent probes. Multi-color labeling are required to label various cell types and structures, which may be difficult under conditions such as in vivo labeling. Stimulated Raman scattering microscopy (SRS) is a burgeoning label-free biological imaging technique that has been used in many areas, such as tumor detection, pharmacokinetics, and neuroscience. Here, we developed a method of label-free imaging of various cell types and structures in lymph nodes with SRS. Collagenous fibers in the lymph node capsule, subcapsular sinus macrophages, B cells, blood vessels and white blood cells were observed in fresh lymph nodes. Based on the visualization of lymph node structure, we prospected its applications in cancer research, aging research and extracellular matrix research.

Keywords: Stimulated Raman scattering, lymph node, label-free imaging, lymphocyte

1. INTRODUCTION

The optical microscopy has been a powerful imaging tool for biomedical research. It allows observing biological processes at different levels from nanometer to micrometer. Fluorescence microscopy, including laser scanning confocal microscopy, multiphoton microscopy, light-sheet microscopy, super-resolution microscopy, etc., has been widely used in biological applications. With the rapid development of fluorescence proteins and fluorescent dyes, the fluorescence microscopy achieves high sensitivity and specificity. However, it is not available to image biomolecules smaller than the fluorescent proteins and fluorescent dyes. That is why label-free imaging techniques were developed.

The spontaneous Raman microspectroscopy is a label-free chemical imaging technique. However, the spontaneous Raman scattering signal is very weak, limiting its imaging speed in biological applications. Coherent Raman scattering microscopy, including coherent anti-Stokes Raman scattering microscopy (CARS) and stimulated Raman scattering microscopy (SRS), is an alternative label-free chemical imaging technique. The coherent Raman scattering signals could be up to 10^7 higher than spontaneous Raman scattering signals. Thus, it allows high-speed bio-imaging. CARS has non-resonant background signals. The Raman spectrum measured by CARS is different from spontaneous Raman scattering spectrum, limiting the application of this technique. SRS is free of non-resonant background signals and has the same Raman spectrum with spontaneous Raman scattering. SRS was developed in 2008 [1] and developed rapidly in the past decade. Video-rate SRS [2], multi-color SRS [3, 4], multiplex SRS [5], fiber-laser SRS [6], volumetric SRS [7, 8], electronic pre-resonance SRS [9] and other modality of SRS were developed. It has also been used widely in biological

*sunneyxie@pku.edu.cn; phone 86 10 62752373

Optics in Health Care and Biomedical Optics IX, edited by Qingming Luo, Xingde Li, Ying Gu, Yuguo Tang, Dan Zhu, Proc. of SPIE Vol. 11190, 111900J · © 2019 SPIE
CCC code: 0277-786X/19/$21 · doi: 10.1117/12.2536264

research, such as tumor biology [10-12], metabolic research [13, 14], neurobiology [15-17], nucleic acids research [18, 19], pharmaceuticals [20, 21] and plant research [22, 23], etc. SRS imaging probes were also developed based on the isotope [24], small molecules [25] and triple-bond [26], etc.

Lymph nodes are an important secondary lymphoid organ in the lymphatic system. It acts as the key site for the initiation of adaptive immune response. Thus, it is related to many biological processes. To image various types of cells and vessels in lymph nodes, it is necessary to label the target with specific antibodies or staining chemicals. For pathology, lymph nodes need to be fixed and sectioned with a microtome. It is difficult to get the 3D information of target cells. For intravital imaging, in vivo fluorescent labeling or transgenic mice is needed. The procedure is usually complicated, expensive and time-consuming. Label-free imaging methods seem promising for imaging lymph nodes both in vitro and in vivo. Up to now, SRS has not been applied in bio-imaging of lymph nodes. Here, we investigated the feasibility of label-free imaging for lymph nodes with SRS. We focused on the imaging the structures and cells that were easy to distinguish by their location and morphology. It could thus avoid complex verification by labeling them with specific antibodies. Collagenous fibers were first imaged because it was in the capsule of the lymph node. The subcapsular sinus macrophages were also the target we imaged since they were at the lymph-tissue interface in the lymph node and was drawing increasing popularity [27, 28]. The germinal centers where B cells resided were also of interest. 3D images of blood vessels and image montages were acquired to display the structure of lymph nodes.

2. MATERIALS AND METHODS

2.1 Stimulated Raman scattering microscopy

SRS imaging was performed with a home-built SRS imaging system equipped with either a picosecond laser or a femtosecond laser as the light source. In the picosecond system, the picosecond laser (APE PicoEmerald, Germany) outputted synchronized pump and Stokes beams. The pump beam was an 80 MHz pulse train with 2 ps pulse width, and tunable from 700 nm to 990 nm. The Stokes beam was 1031 nm and modulated by a built-in electro-optic modulator (EOM) at 20 MHz. Two beams were overlapped and coupled into an upright laser-scanning microscope (Olympus FVMPE-RS, Japan). SRS signals were detected by a customized photodiode and lock-in amplifier module (APE PicoEmerald, Germany). In the femtosecond system, the femtosecond laser (Spectra-Physics Insight DeepSee, USA) outputted a tunable pump beam (680-1300 nm) and fixed Stokes beam (1040 nm) at an 80 MHz repetition rate. The Stokes beam was modulated by an electro-optic modulator (EOM) at 10 MHz. The pump and Stokes beams were chirped with high-density glass rods. They were then overlapped and coupled into an upright laser-scanning microscope (Olympus FV300, Japan). SRS signals were detected by a photodiode and a home-made lock-in amplifier. A 25X water-immersion objective lens optimized for near infrared laser was used for imaging. Images were acquired at a size of 512 × 512 pixels. The pixel dwell time is 2 μs or 4 us. Each image was line-averaged by 3 to 5 times to get a final image. For the purpose of image montaging, an image stack was acquired by a motorized stage and an automatic control software. There was 10% overlap between two neighboring images in the image stack. The z-stack images were acquired with a 1 μm-depth step.

Three channels were selected to image protein, lipid and off-resonance background at 2926 cm^{-1}, 2850 cm^{-1} and 2700 cm^{-1}, respectively. In the picosecond system, the pump laser was tune to 792.5 nm, 797.2 nm and 806.5 nm, respectively. In the femtosecond system. The pump laser was tuned to 797.4 nm, 802.2 nm and 812.0 nm, respectively.

2.2 Image processing

SRS images were processed with ImageJ and Imaris software. The “BioFormats” plugin in ImageJ was used to open .oir files acquired by the Olympus microscope and converted them into .tiff images. Since the illumination of an image might not be even, each image in the image stack was divided by a background frame to reduce the unevenness. The "Stitching" plugin was used to align and stitch the image stack to create a single high-resolution montage[29]. Pseudo colors were used in merged images of different channels. Reconstruction of 3D images was performed with the Imaris software.

2.3 Tissue samples

Fresh lymph nodes were collected from 4-10 weeks-old C57 or Balb/c mice. The fat on the surface of lymph nodes was removed carefully under a stereoscope. The lymph node was positioned on a home-made glass slide that had a hole to hold phosphate buffer saline. A cover glass slide was sealed to the glass to keep the lymph node from moving.

3. RESULTS AND DISCUSSIONS

3.1 Structure of the lymph node

To image the structure of lymph nodes, we first focused on the capsule that is composed of dense irregular connective tissue and collagenous fibers. It was found that SRS is very sensitive to the collagenous fibers in the protein channel at 2925 cm^{-1} (Figure 1A). However, there was no signal of collagenous fibers in the lipid channel at 2850 cm^{-1} (Figure 1B).

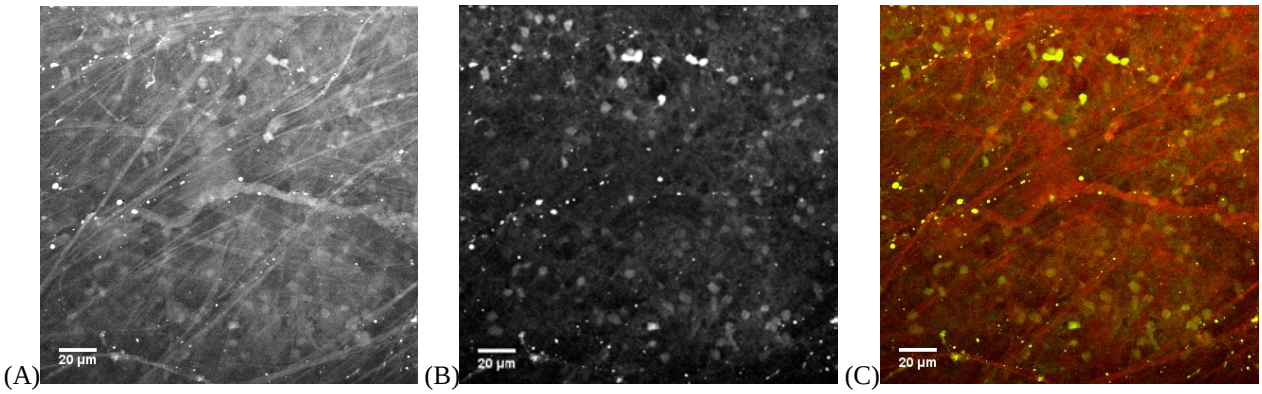

Figure 1. SRS images of collagenous fibers in the capsule of a lymph node. (A) The protein channel was imaged at 2925 cm^{-1}. (B) The lipid channel was imaged at 2850 cm^{-1}. (C) Merged image of the protein (red) and lipid (green) channels. The scale bars are 20 μm.

Underneath the capsule of the lymph node, it is the subcapsular sinus that contains a few macrophages. We observed subcapsular sinus macrophages in the lipid channel at 2850 cm^{-1} (Figure 2). The macrophaegs were bigger than the dense cells and had many droplets inside them that had strong signals in the lipid channel. These signals might come from engulfed cellular debris by the subcapsular macrophages.

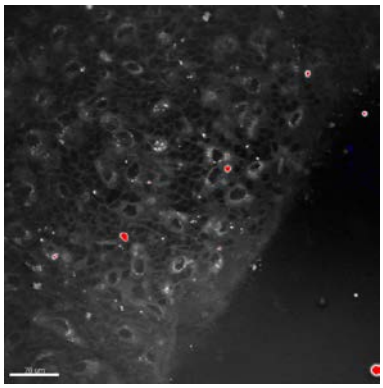

Figure 2. SRS image of subcapsular sinus macrophages in a fresh inguinal lymph node of a 6-week-old mouse in the lipid channel imaged at 2850 cm^{-1}. The bigger cells in this image were macrophages. The scale bar is 20 μm.

The germinal center is the major site that B cells reside. A germinal center was located by its anatomical structure and imaged with SRS. It was found that most cells were dense B cells (Figure 3). It should be noted B cells and T cells had quite similar morphology and chemical components. It was difficult to distinguish them by SRS imaging. We thought that most cells in Figure 3 were B cells because few T cells might enter the germinal center. There were also many bright cells in two channels that might be dead cells.

The off-resonance channel at 2700 cm^{-1} was used to image blood vessels. The blood had strong signals due to light absorption, whereas cells had weak signals in the protein and lipid channels. The 3D images of partial blood vessels were reconstructed (Figure 4). Some black holes (Figure 4B) were found that might be white blood cells because they had much less light absorption than the blood.

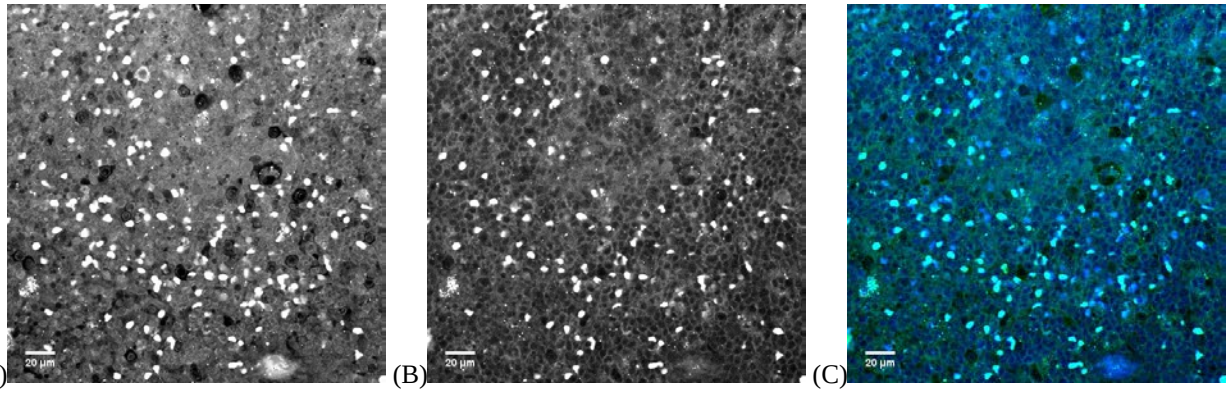

Figure 3. SRS images of the germinal center in the protein channel (A) and lipid channel (B) at 2925 cm^{-1} and 2850 cm^{-1} respectively. In the merged image (C), the green was for lipid and the blue was for protein. The scale bars are 20 μm.

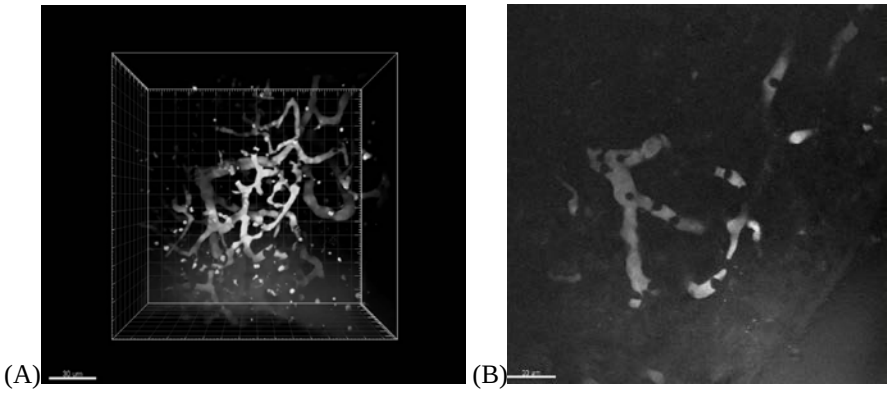

Figure 4. SRS image of blood vessels in a fresh lymph node in the off-resonance channel at 2700 cm^{-1}. (A) Reconstructed 3D images. (B) SRS image in which the black holes were white blood cells. The scale bars are 30 μm (A) and 20 μm (B), respectively.

To get a full view of the lymph node, montage images were also acquired in the protein and lipid channels (Figure 5). Some dark areas which might be germinal centers could be found. Other structures of interest could be enlarged for observation.

3.2 Potential application

Based on the label-free imaging of fresh Lymph nodes, we are able to apply this method in various research. The lymph node is a site of cancer metastasis. With SRS imaging, it is possible to detect tumor cells without labeling. Tumor cells have different morphology and chemical components from normal cells in the lymph node. Thus, this label-free imaging method could be applied in many types of cancers. Among cancers, melanoma is special for SRS imaging since there is melanin in melanoma cells. Melanin has strong light absorption and generates strong signals. Although these signals are not entirely SRS signals, it is specific for melanoma cells. Therefore, melanoma would be a good target cancer type for SRS imaging.

Age-dependent histoarchitectural changes in lymph nodes is a potential area that SRS imaging should be focused on. In lymph nodes, germinal centers are common in infants and children, decrease in adults and absent in the elderly [30]. Hyaline, lymphocyte depletion and fibrosis are also related to aging. We have imaged some lymph nodes at different ages and found similar results with unknown knowledge (Data not shown).

Lymph nodes contain an extensive array of extracellular matrix fibers, which are primarily collagen [31]. There is evidence supporting that the extracellular matrix as a pathway for lymphocyte migration [32] and other important biological functions. SRS is very sensitive to these collagenous fibers, providing a powerful tool to study in this area. We are now investigating the relationship between the extracellular matrix and macrophage migration.

(A) 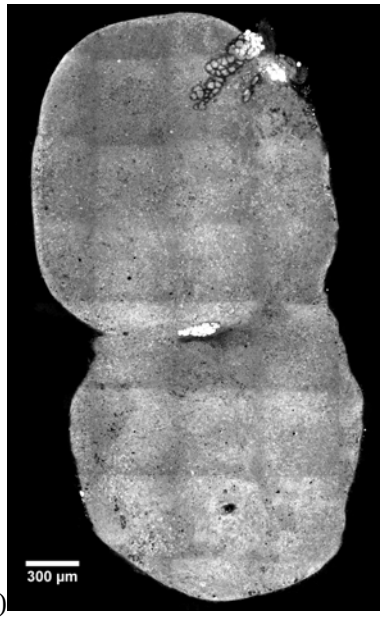

(B) 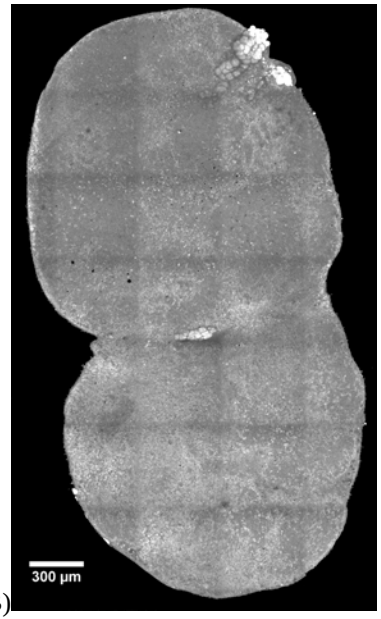

Figure 5. SRS image montages of a lymph node in the protein (A) and lipid channels (A). The scale bars are 300 μm.

3.3 Discussion

In this work, SRS images were acquired in fresh murine lymph nodes with the transmission mode (Trans-SRS). It is practical to perform SRS imaging with epi- mode (epi-SRS) by using a quarter-wave plate and polarizing beam splitter to collect backward photons. The signal of epi-SRS is weaker than trans-SRS, but could be improved by using a large-area ring-shaped detector placed between the objective and the sample. With epi-SRS, it is feasible to image lymph nodes in vivo.

The maximum SRS imaging depth in this work was about 150 μm, comparable to multi-photon microscopy. It was very important to remove the fat on the lymph node, which could significantly affect the SRS imaging depth. To increase the maximum imaging depth, optical tissue clearing is a practical method for in vitro imaging. Volumetric SRS is suitable for fast imaging of lymph nodes on a large scale but would sacrifice the spatial resolution.

In this work, various types of cells and structures in lymph nodes were distinguished mainly by their anatomical location and morphology. Thus, only very limited cells and structures were distinguished. There were many un-distinguished cells and structures in SRS images. It is necessary to distinguish them and verify with specific antibodies.

ACKNOWLEDGEMENTS

The authors thank Dr. Yinghui Zheng and Dr. Longzhi Tan for donating mouse lymph nodes, Dr. Shuang Geng for constructive discussion. Yuanzhen Suo is supported by the China Postdoctoral Science Foundation (2018M641096).

REFERENCES

[1] Freudiger, C. W., Min, W., Saar, B. G. *et al.*, "Label-free biomedical imaging with high sensitivity by stimulated Raman scattering microscopy," Science Papers 322(5909), 1857-1861 (2008).
[2] Saar, B. G., Freudiger, C. W., Reichman, J. *et al.*, "Video-rate molecular imaging in vivo with stimulated Raman scattering," Science Papers 330(6009), 1368-1370 (2010).
[3] Yang, W., Li, A., Suo, Y. *et al.*, "Simultaneous two-color stimulated Raman scattering microscopy by adding a fiber amplifier to a 2 ps OPO-based SRS microscope," Opt. Lett. Papers 42(3), 523-526 (2017).
[4] Lu, F.-K., Ji, M., Fu, D. *et al.*, "Multicolor stimulated Raman scattering (SRS) microscopy," Mol. Phys. Papers 110(15-16), 1927-1932 (2012).
[5] Fu, D., Lu, F.-K., Zhang, X. *et al.*, "Quantitative chemical imaging with multiplex stimulated Raman scattering microscopy," J. Am. Chem. Soc. Papers 134(8), 3623-3626 (2012).

[6] Freudiger, C. W., Yang, W., Holtom, G. R. *et al.*, "Stimulated Raman Scattering Microscopy with a Robust Fibre Laser Source," Nat. Photonics Papers 8(2), 153-159 (2014).
[7] Chen, X., Zhang, C., Lin, P. *et al.*, "Volumetric chemical imaging by stimulated Raman projection microscopy and tomography," Nat. Commun. Papers 8(1), 15117 (2017).
[8] Wei, M., Shi, L., Shen, Y. *et al.*, "Volumetric chemical imaging by clearing-enhanced stimulated Raman scattering microscopy," Proc. Natl. Acad. Sci. USA Papers 116(14), 6608-6617 (2019).
[9] Wei, L., Chen, Z., Shi, L. *et al.*, "Super-multiplex vibrational imaging," Nature Papers 544(7651), 465-470 (2017).
[10] Ji, M., Orringer, D. A., Freudiger, C. W. *et al.*, "Rapid, label-free detection of brain tumors with stimulated Raman scattering microscopy," Sci.Transl. Med. Papers 5(201), 201ra119-201ra119 (2013).
[11] Ji, M., Lewis, S., Camelo-Piragua, S. *et al.*, "Detection of human brain tumor infiltration with quantitative stimulated Raman scattering microscopy," Sci.Transl. Med. Papers 7(309), 309ra163-309ra163 (2015).
[12] Ji, M., Yang, Y., and Chen, L., "Stimulated Raman scattering microscopy for rapid brain tumor histology," J. Innov. Opt. Health. Sci. Papers, (2017).
[13] Yue, S., Li, J., Lee, S.-Y. *et al.*, "Cholesteryl ester accumulation induced by PTEN loss and PI3K/AKT activation underlies human prostate cancer aggressiveness," Cell Metab. Papers 19(3), 393-406 (2014).
[14] Wang, M. C., Min, W., Freudiger, C. W. *et al.*, "RNAi screening for fat regulatory genes with SRS microscopy," Nat. Methods Papers 8(2), 135-8 (2011).
[15] Tian, F., Yang, W., Mordes, D. A. *et al.*, "Monitoring peripheral nerve degeneration in ALS by label-free stimulated Raman scattering imaging," Nat. Commun. Papers 7, 13283 (2016).
[16] Fu, D., Yang, W., and Xie, X. S., "Label-free Imaging of Neurotransmitter Acetylcholine at Neuromuscular Junctions with Stimulated Raman Scattering," J. Am. Chem. Soc. Papers 139(2), 583-586 (2017).
[17] Ji, M., Arbel, M., Zhang, L. *et al.*, "Label-free imaging of amyloid plaques in Alzheimer's disease with stimulated Raman scattering microscopy," Sci. Adv. Papers 4(11), eaat7715 (2018).
[18] Lu, F.-K., Basu, S., Igras, V. *et al.*, "Label-free DNA imaging in vivo with stimulated Raman scattering microscopy," Proc. Natl. Acad. Sci. USA Papers 112(37), 11624-11629 (2015).
[19] Zhang, X., Roeffaers, M. B., Basu, S. *et al.*, "Label-free live-cell imaging of nucleic acids using stimulated Raman scattering microscopy," Chemphyschem Papers 13(4), 1054-9 (2012).
[20] Fu, D., Zhou, J., Zhu, W. S. *et al.*, "Imaging the intracellular distribution of tyrosine kinase inhibitors in living cells with quantitative hyperspectral stimulated Raman scattering," Nat. Chem. Papers 6(7), 614-622 (2014).
[21] Saar, B. G., Contreras-Rojas, L. R., Xie, X. S. *et al.*, "Imaging drug delivery to skin with stimulated Raman scattering microscopy," Mol. Pharm. Papers 8(3), 969-75 (2011).
[22] Saar, B. G., Zeng, Y., Freudiger, C. W. *et al.*, "Label-Free, Real-Time Monitoring of Biomass Processing with Stimulated Raman Scattering Microscopy," Angew. Chem. Int. Ed. Papers 49(32), 5476-5479 (2010).
[23] Man, Y., Zhao, Y., Ye, R. *et al.*, "In vivo cytological and chemical analysis of Casparian strips using stimulated Raman scattering microscopy," J. Plant Physiol. Papers 220, 136-144 (2018).
[24] Wei, L., Yu, Y., Shen, Y. *et al.*, "Vibrational imaging of newly synthesized proteins in live cells by stimulated Raman scattering microscopy," Proc. Natl. Acad. Sci. USA Papers 110(28), 11226-11231 (2013).
[25] Hu, F., Zeng, C., Long, R. *et al.*, "Supermultiplexed optical imaging and barcoding with engineered polyynes," Nat. Methods Papers 15, 194 (2018).
[26] Hong, S., Chen, T., Zhu, Y. *et al.*, "Live-cell stimulated Raman scattering imaging of alkyne-tagged biomolecules," Angew. Chem. Int. Ed. Papers 53(23), 5827-31 (2014).
[27] Iannacone, M., Moseman, E. A., Tonti, E. *et al.*, "Subcapsular sinus macrophages prevent CNS invasion on peripheral infection with a neurotropic virus," Nature Papers 465(7301), 1079-1083 (2010).
[28] Moran, I., Grootveld, A. K., Nguyen, A. *et al.*, "Subcapsular Sinus Macrophages: The Seat of Innate and Adaptive Memory in Murine Lymph Nodes," Trends in Immunology Papers 40(1), 35-48 (2019).
[29] Preibisch, S., Saalfeld, S., and Tomancak, P., "Globally optimal stitching of tiled 3D microscopic image acquisitions," Bioinformatics Papers 25(11), 1463-1465 (2009).
[30] Tsakraklides, V., Tsakraklides, E., and Good, R. A., "An autopsy study of human axillary lymph node histology," Am J Pathol Papers 78(1), 7-22 (1975).
[31] Kramer, R. H., Rosen, S. D., and McDonald, K. A., "Basement-membrane components associated with the extracellular matrix of the lymph node," Cell Tissue Res. Papers 252(2), 367-375 (1988).
[32] Sobocinski, G. P., Toy, K., Bobrowski, W. F. *et al.*, "Ultrastructural localization of extracellular matrix proteins of the lymph node cortex: evidence supporting the reticular network as a pathway for lymphocyte migration," BMC Immunol. Papers 11(1), 42 (2010).